Journal of Biomedical Optics

BiomedicalOptics.SPIEDigitalLibrary.org

Measurement of the retinal arteriolar response to a hyperoxic provocation in nonsmokers and smokers, using a high-resolution confocal scanning laser ophthalmoscope

Margaret O' Halloran
Eamonn O'Donoghue
Chris Dainty

SPIE.

Measurement of the retinal arteriolar response to a hyperoxic provocation in nonsmokers and smokers, using a high-resolution confocal scanning laser ophthalmoscope

Margaret O' Halloran,[a,*] Eamonn O'Donoghue,[b] and Chris Dainty[c]
[a]National University of Ireland Galway, Applied Optics Group, School of Physics, Galway, Ireland
[b]University Hospital Galway, Ophthalmology Department, Galway, Ireland
[c]University College London, Institute of Ophthalmology, 11–43 Bath Street, London EC1V 9EL, United Kingdom

Abstract. We used a high-resolution confocal scanning laser ophthalmoscope to measure the magnitude of change in retinal arteriolar diameters in response to oxygen breathing in young, healthy nonsmokers and smokers. Image sequences were obtained before and during oxygen breathing. Image sequences were desinusoided, registered, and averaged, before vessel diameters were measured using a sliding linear regression filter. Arteriole diameters were observed to constrict during the first 5 min. of oxygen breathing, plateau, and remain stable while hyperoxia was maintained, returning to baseline at the end of the hyperoxic period. Blood flow to the temporal retina was found to be higher than to the nasal retina ($p = 0.008$). The percentage constriction of vessels did not vary across retinal quadrants ($p = 0.372$, analysis of variance) and did not depend on vessel size ($p = 0.538$). Baseline diameters were unaffected by acute cigarette smoking. The magnitude of vasoconstriction was diminished in smokers compared to nonsmokers ($p = 0.017$), while acute smoking did not influence the percentage constriction attained by the vessels ($p = 0.621$). Using a high-resolution imaging technique allowed us to measure reactivity to a high degree of accuracy and to assess it in vessels of smaller caliber than were previously studied. [DOI: 10.1117/1.JBO.19.7.076012]

Keywords: retina; vascular reactivity; hyperoxia; retinal vessel diameter; endothelium; smoking; scanning laser ophthalmoscope; high-resolution imaging.

Paper 140309R received May 15, 2014; revised manuscript received Jun. 10, 2014; accepted for publication Jun. 11, 2014; published online Jul. 14, 2014.

1 Introduction

The endothelium is a monolayer of cells that lines the inner surface of blood vessels; it participates in vascular permeability, platelet activity, and coagulation.[1,2] It also plays an important role in local blood flow regulation by secreting vasoactive factors, which modulate vascular tone, in response to disturbances in perfusion pressure or alterations in metabolism, to ensure an adequate blood supply to the tissue.[2] Vascular reactivity is defined as the magnitude of change in a hemodynamic parameter (e.g., vessel diameter, blood flow velocity, volumetric blood flow) in response to an artificial disturbance (provocation) in perfusion pressure, metabolism, or blood gas concentration.[3] Therefore, measuring vascular reactivity provides us with the opportunity to assess endothelial function. There has been growing interest in the study of endothelial function since it was found to be impaired in several cardiovascular diseases, such as hypertension and diabetes.[2] Reliable assessment of endothelial function could improve understanding and could potentially facilitate early diagnosis, risk prediction, and treatment monitoring in these diseases.

Vascular reactivity can be directly visualized in the retina and has been assessed using a number of provocation methods, including isometric exercise,[4–6] postural change,[7] intraocular pressure (IOP) elevation,[8] flickering light,[9–12] and blood gas perturbations.[13–16] For our experiments, we decided to use oxygen breathing as the provocation stimulus to evoke a retinal vascular reaction. This stimulus method was chosen because oxygen breathing induces minimal discomfort and anxiety in the subjects, and also poses minimal risk to their well-being. A variety of measurement techniques have also been used to assess retinal vascular reactivity, including fundus camera,[4,7,17,18] blue field entoptic technique,[15,19] laser Doppler velocimetry,[4,15,18] laser speckle technique,[20,21] retinal vessel analyzer (RVA),[11,12,14,15,22] and Canon laser blood flowmeter (CLBF).[3,23,24] Blood flow is proportional to the fourth power of the vessel radius; this underlines the importance of accurately measuring changes in vessel diameter when studying blood flow regulation. However, the quantification of vessel caliber changes has been limited by the resolution of techniques used to date, with previous studies assessing vessels measuring ≥ 80 μm.[25,26] To our knowledge, high-resolution imaging techniques have thus far not been utilized to measure vessel diameter changes in reactivity studies. The motivation behind this study was to measure the magnitude of retinal vascular constriction in response to hyperoxia, using a high-resolution confocal scanning laser ophthalmoscope (SLO) and image processing techniques in a bid to assess retinal vascular reactivity to a high degree of accuracy and to measure it in vessels of smaller caliber than the resolution of previous measurement techniques allowed.

*Address all correspondence to: Margaret O'Halloran, E-mail: margaret.ohalloran@gmail.com

0091-3286/2014/$25.00 © 2014 SPIE

A comprehensive understanding of retinal reactivity in healthy subjects and any factors that affect it is needed to study disturbances in pathology. However, studies have reported contradictory results in relation to many of the investigated factors hypothesized to influence the vascular response to stimuli. It is imperative to understand whether the reactivity response to stimuli is independent of arteriolar size and retinal region in order to know if it is possible to draw conclusions about the reactivity of the whole of the retinal vasculature from a single, arbitrary measurement site. It is also necessary to know how chronic and acute smoking affect the vascular reactivity response. The following experiments were performed to validate the use of our imaging system in reactivity studies by making measurements of some established results and comparing our findings with the literature data. It was also our aim to help clarify previous equivocal results by adding to the data of more controversial areas.

2 Methods

2.1 *Retinal Imaging*

Retinal imaging was performed with a manufacturer-modified Heidelberg Retina Tomograph (HRT)-classic (Heidelberg Engineering, Heidelberg, Germany), which is a confocal SLO. The modified HRT-classic could originally image with a 20, 15 or 10 deg field of view (FOV), but it was modified such that it could image at smaller FOVs of 10, 2, or 1 deg. Thus, it is capable of very high-resolution imaging of the retina. Images taken at each FOV of the modified HRT-classic can be seen in Fig. 1. Images are 256×256 pixels. Ocular refraction can affect image magnification, but each pixel subtends ~ 10 μm at 10 deg FOV, 2 μm at 2 deg FOV, and 1 μm at 1 deg FOV. For the assessment of the reactivity, response to hyperoxia subjects were imaged at 2 deg FOV.

The modified HRT-classic images using a 675-nm diode laser. During image acquisition, at any given instant, only one point on the retina is illuminated. Therefore, to acquire a two-dimensional image, the emitted light beam must be swept over the retina. The emitted beam is scanned in the x and y axes along the plane of focus perpendicular to the optic axis (z axis) using two oscillating mirrors.[27] In this way, an image is recorded point-by-point, over time, as the region of interest is scanned in a raster-like fashion. The fast scan is in the horizontal direction, with a scanning rate of 8 kHz, while the vertical scan rate is 30 Hz. It scans in double-scan mode, which means that the first line is recorded as the scanner moves from left to right and the second line is acquired as the beam scans back from right to left. Thus, two lines of an image are obtained in one complete cycle of the fast horizontal scanner.[27]

This system has optical sectioning capabilities; however, image sequences of 32 frames were acquired at a single focal plane to obtain a video of the vasculature. The acquisition time for a single frame was 32 ms, while the acquisition time for a sequence of 32 frames was 1.5 s, with a resetting time of 16 ms between frames.

The fixation target used was a Samsung Galaxy Tab™ (Seoul, Republic of Korea), which displayed a red dot that could be altered in size and moved around the screen by the investigator to center the retinal region of interest in the captured image. Subjects fixated on the target with the eye opposite to the one being imaged.

2.2 *Desinusoiding and Image Registration*

Raw videos were first processed to correct for distortions due to raster scanning. The SLO employs a sensor that captures pixels at a constant rate and a resonant scanner whose velocity varies sinusoidally across each scan line. This results in a horizontal distortion in raw videos. The velocity of the scanner is slowest at the edges of the frame and fastest in the center; accordingly, more pixels are recorded per retinal area toward the edges compared to the center of the image. Videos of a calibration grid were used to estimate this horizontal warping, and a desinusoiding algorithm was developed in MATLAB® to correct for this distortion. Briefly, the algorithm used a cost function, whose value was high when the lines of the calibration grid in the image were irregularly spaced and low (close to zero) when evenly spaced, and the Nelder-Mead simplex search algorithm to calculate the transformation necessary to dewarp the images.

The next step was image stabilization to correct for eye motion to allow for image averaging to produce a high signal-to-noise retinal image. The eye is constantly moving, even during attempts to fixate steadily on a stationary target. All retinal imaging systems suffer from these eye movements; however, these distortions are particularly apparent in adaptive optics ophthalmic instruments and the modified HRT-classic, as the distortion scales with the magnification of the instrument.[28–30] Eye motion that occurs during the acquisition of

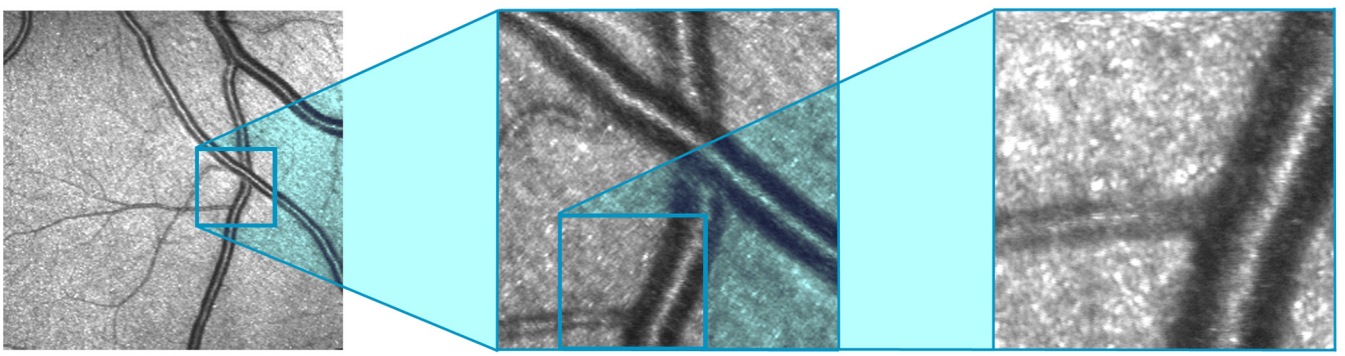

Fig. 1 Images of the same portion of the retina taken at different fields of view (FOV) of the modified HRT-classic. (a) 10 deg FOV, (b) 2 deg FOV, and (c) 1 deg FOV.

image sequences acquired by scanning techniques produces distortions that are unique in each frame because the images are captured over time from a scanning focused beam. These distortions can be extreme if a microsaccade occurs during acquisition, as can be seen in Fig. 2. Therefore, registration of retinal images acquired using scanning techniques is more complex than implementing a simple rigid translation to align the images. However, during short time intervals, retinal motion can be well approximated by a simple translation. (Note that if the images have not been properly desinusoided, this assumption is not valid—desinusoiding is essential before registration.) This has led to patch-based correlation methods being used to register small-FOV SLO images.[28,29,31] We implemented such a patch-based registration scheme to align our image sequences. Because the direction of the fast scan in the SLO is horizontal, it is assumed that a single horizontal scan line is unaffected by fixational eye motion and is essentially a snapshot of the retina. Ideally, each patch would have extended just one line vertically (the direction of the slow scanner); however, in most sequences, such patches fail to register due to noise. A compromise between having enough data to reliably match the patches and obtaining the most accurate within-frame motion estimates must be reached. Thus, each template image was partitioned into patches that extend horizontally across the entire image but extend to just a few lines of the vertical extent of the image.

The correlation coefficient computed in the frequency domain, as described in a paper by Lewis,[32] was the match metric used in the MATLAB®-based algorithm to register sequences of images from the HRT. It is necessary to use the correlation coefficient to make shift estimations robust to intensity fluctuations. Such intensity fluctuations are very common in image sequences obtained from ophthalmoscopes due to subject misalignment, tear film break-up, etc. Another useful property of the correlation coefficient is that it has an absolute range $[-1, 1]$. This was used to delete frames that did not sufficiently match the reference image by discarding images whose maximum correlation coefficient did not reach a set threshold. This could be due to insufficient overlap between the reference and template images, which occurred when the eye wandered too far away from the fixation target, or due to extreme warping in the template image. Before importing the desinusoided image sequence into the registration algorithm, frames where blinks had occurred, resulting in the intensity dropping to zero in the images throughout the blink, were manually deleted.

The first step in our registration algorithm was to implement a full-image alignment. The images underwent a full-image registration, before applying the patch-based scheme, as our images were small, extending just 256 pixels horizontally, and therefore, removing the interframe eye-motion made the patch-based, intraframe registration more robust. The first image in a sequence was normally taken as the reference image, unless it showed visible signs of distortion. The same image was used as the reference image in the full-image and patch-based registration steps.

Once the images were registered, high-signal-to-noise images were obtained by averaging the sequence of images. Figure 3 shows single frames and temporal averages of registered sequences. An improvement in signal-to-noise in the average image, Fig. 3(b), compared to the single image, Fig. 3(a), is evidence of the registration accuracy. In Fig. 3(c), noise was not as prevalent and individual photoreceptors can be distinguished; the corresponding average image, Fig. 3(d), shows no loss of detail, which would occur if the images were not accurately registered.

2.3 *Vessel Tracking and Diameter Measurement*

A semiautomated vessel tracking and diameter measurement method was implemented. This method was based on the assumption that an arteriole can be considered as a curved cylinder consisting of a linkage of many small, straight cylinders. The MATLAB®-based algorithm commenced by importing an averaged image of an arteriolar segment. A low-pass Gaussian filter was applied to the average image to reduce sharp transitions in background luminance. The smoothed image was then displayed and the user selected n seed points, sp_n, at the center of the vessel describing the path of the vessel. The seed points were selected such that the section of vessel between two successive seed points was approximately straight. Using these seed points, the vessel was then divided into $n-1$ segments, where $\mathrm{segment}_n$ consisted of the interval $[\mathrm{sp}_n, \mathrm{sp}_{n+1}]$. The direction of each segment, α_n, was calculated. Estimated center points, cp, were calculated along the segment. Estimated center points were calculated to be 2 pixels apart in the segment direction α_n.

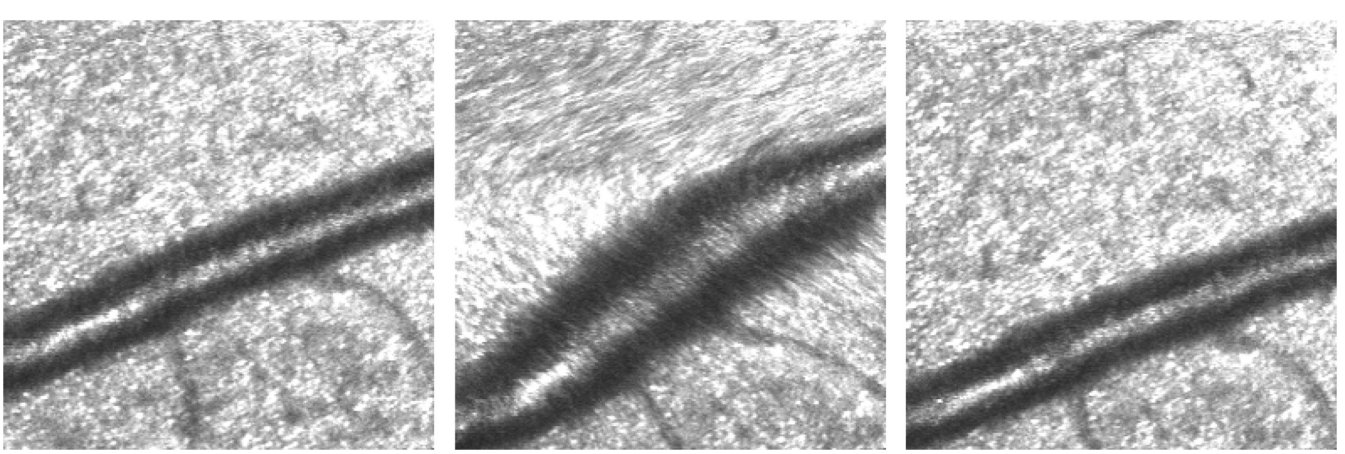

Fig. 2 Example of extreme distortion that can occur when using scanning techniques. Three sequential images taken from a sequence obtained by the modified HRT-classic are shown. The second image shows severe distortion due to a microsaccade, which occurred during image acquisition.

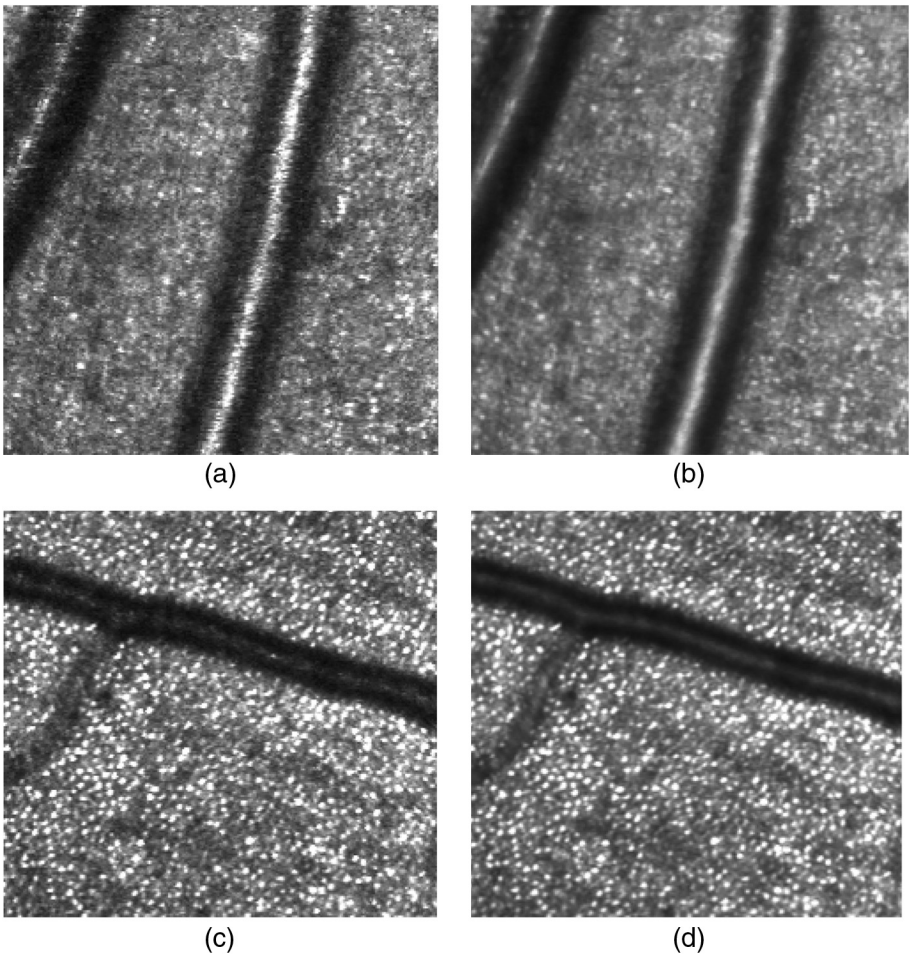

Fig. 3 Left: (a) and (c) are single frames of image sequences obtained from the modified HRT-classic. Right: (b) and (d) are the temporal averages of the image sequences after registration. In both of these examples, all 32 frames of the image sequences were retained after image registration and used in the image averaging step.

A cross-section line was calculated at each center point, perpendicular to the segment direction and centered at the center point, Fig. 4(a). A vessel profile, Fig. 4(b)(i), was then extracted at each cross-section line.

The vessel edges and center positions were identified using a sliding linear regression filter method proposed by Chapman et al.[33] This technique is based on fitting a best fit line by linear regression relating image intensity against distance along the profile within a sliding window filter. The window of W points centered on the i'th point was progressively moved point-by-point along the profile, as demonstrated in Fig. 4(b)(i). At each point, a straight line was fit to the intensity values within the window using the least-squares method. The gradient of the straight line was recorded at each point, m_i. Figure 4(b)(ii) shows the corresponding gradient data of the vessel profile. The edge points were determined from this gradient data. The left edge was taken as the minimum slope obtained from the left half of the profile. The right edge was taken as the maximum slope obtained for the right half of the profile. The actual center points of the vessel were found by taking the central portion of the vessel profile and locating the point at which the gradient changed from positive to negative. This process is demonstrated in Fig. 4(b). Vessel diameters were then set as the distance between corresponding left and right edges, giving a diameter value for each center point. The median of these vessel widths was taken as the vessel diameter.

In this method, one needs to consider the window size W. Large window sizes reduce the occurrence of vessel edges being incorrectly located at random bright/dark spots in the background, while short windows provide better edge resolution, especially for small vessels, but at the expense of reduced noise rejection. For this reason, this technique tracked the vessel twice to incorporate adaptation of the size of the filter window to the approximate size of the vessel. During the first time of tracking, an estimate of the vessel edges, center points, and diameters was calculated using a large cross-section line (100 pixels) and a long window length (10 pixels). For the second time of tracking, the length of the cross-section line was set to be only slightly greater than the median diameter, which was estimated in the first run, and a shorter filter was applied ($\sim$10% of the length of the cross-section line). Therefore, during the second run, despite the reduced noise rejection due to the shorter filter length, the edge points were rarely identified at random points in the background. This was because little background intensity was included in the extracted profile due to the cross-section line being adapted to an estimate of the vessel diameter, so there were few random bright/dark spots that could mistakenly have been determined as edge points. The diameter

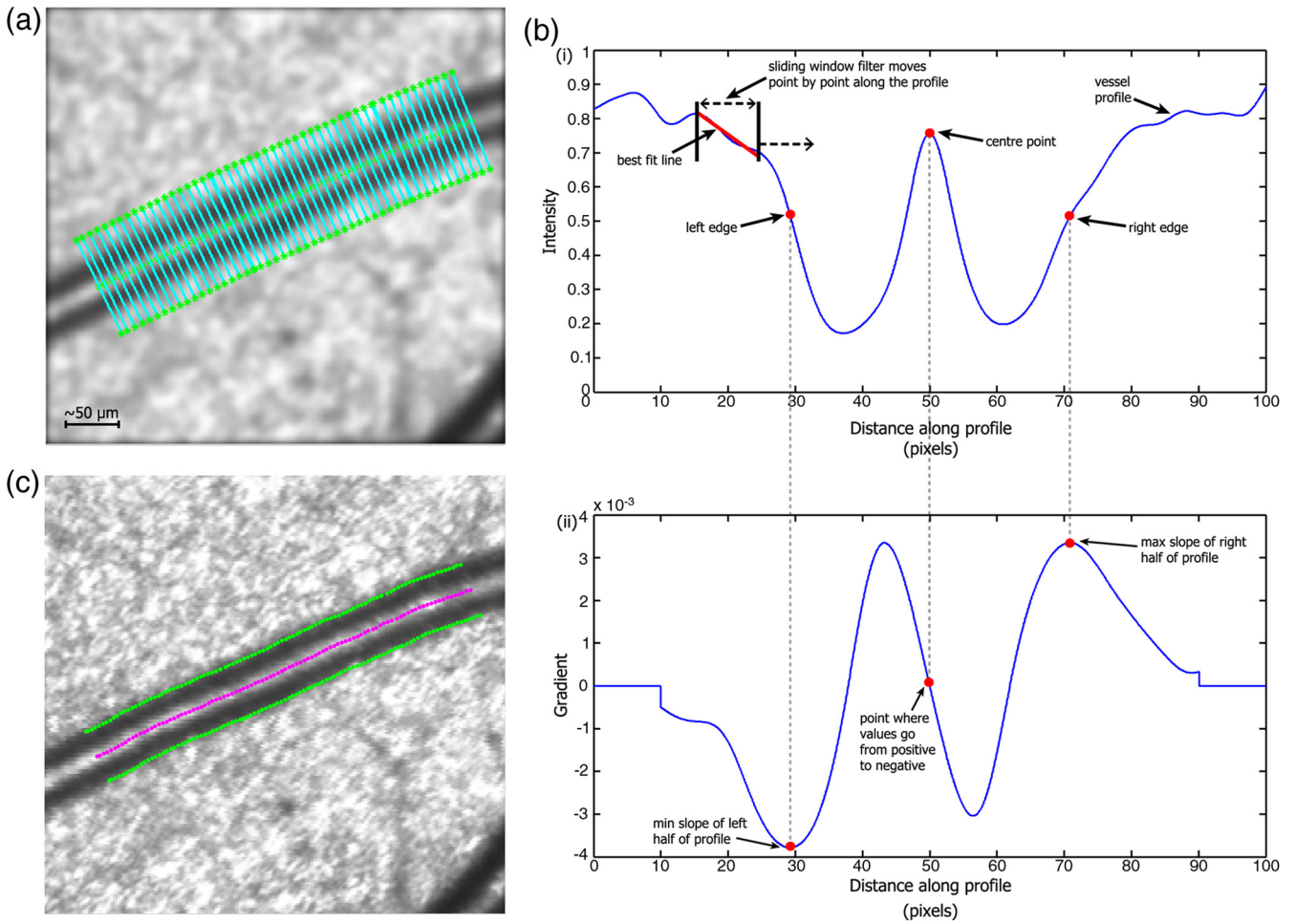

Fig. 4 (a) Estimated center points and cross-section lines. (b) The sliding linear regression filter method was applied to the vessel profiles (i) and the center and edge points were determined from the resulting gradient data (ii). (c) The center and edge points resulting from using this technique.

of the arteriole was set as the median diameter calculated from the second time of tracking.

In Fig. 4(c), the edge points displayed were calculated from the resulting arteriole diameter, centered at the calculated center points and perpendicular to the vessel direction. From this, it can be seen that this method delineates the vessel well and provides a good estimate of the arteriole diameter.

2.4 *Retinal Mosaics*

At small FOVs, it can be difficult to locate vessels of interest and repeatedly return to them for multiple measurements. Therefore, approximately nine 10 deg FOV (the largest FOV of the modified HRT-classic) image sequences were obtained from one eye of each participant and were used to create a mosaic of the retina. An example of one such mosaic can be seen in Fig. 5. The mosaic was used during the reactivity measurements to define suitable measurements sites (relatively straight arteriole segments with good contrast to the background) and to aid the investigator in navigating the retina at a small FOV. Having the mosaic essentially provided the investigator with a map of the retinal vasculature, greatly increasing the speed and efficiency of imaging at high resolution. The mosaic of the 10 deg images was generated by first desinusoiding the images and then combining overlapping images using Adobe Photoshop®.

2.5 *Oxygen Delivery System*

Subjects were administered 100% oxygen via a nonrebreathing system at a flow rate of 12 L/min at atmospheric pressure for ~20 min. The nonrebreathing system consisted of an oxygen cylinder, regulator and flowmeter (which adjust the oxygen flow), and a nonrebreathing mask. A nonrebreathing system ensures a high flow of oxygen and a minimal intake of room air, resulting in an inspired oxygen concentration of 80 to 90%. The subjects were instructed to report any noticed effects of oxygen inhalation; none of the volunteers noted any adverse reaction to oxygen breathing.

3 Experiments

3.1 *Subjects*

Twenty-nine (6 women and 23 men) healthy, normal volunteers (mean age ± SD, 22.1 ± 3.7 years) participated in this study, including 17 (4 women and 13 men) nonsmokers (mean age ± SD, 21.9 ± 2.6 years) and 12 (2 women and 10 men) smokers (mean age ± SD, 22.4 ± 5.1 years). Each subject signed a written consent form after the nature of the study and experiment protocol were explained in detail. All procedures conformed to the tenets of the Declaration of Helsinki and were reviewed and approved by the National University of

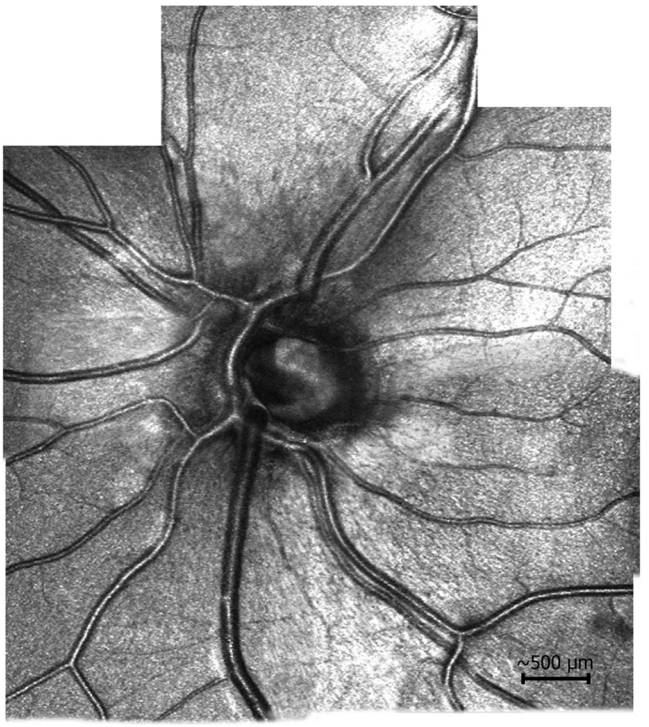

Fig. 5 A typical mosaic, composed of nine 10 deg FOV images.

Ireland, Galway Ethics Committee. Exclusion criteria included ages <18 years or >40 years, unclear optic media, pregnant or breastfeeding women, any cardiovascular or respiratory disorders, taking medication with known effects on blood flow (e.g., muscle relaxants), and taking any chronic medication. Smoking status was identified by self-report. The average number of cigarettes smoked by the smokers per day ranged from 3 to 20 (mean $\pm$ SD, 10.9 ± 6.3 cigarettes), and the duration of smoking varied from 1 to 20 years (mean $\pm$ SD, 6.1 ± 5.7).

3.2 *Experimental Protocol*

Volunteers attended three sessions. The first session was to determine eligibility, to familiarize the subjects with the measurement technique, and to obtain some large-FOV images. These images were used to create the retinal mosaics. One eye from each subject was selected. The magnitude of retinal vascular reactivity in response to the hyperoxic stimulus was measured during the second and third sessions, with intervals of 1 to 17 days between these sessions. Subjects were asked to abstain from alcohol, caffeine, and cigarette smoking (in the case of smokers) for 12 h before study sessions 2 and 3. Subjects rested for at least 5 min before the start of each experiment to stabilize baseline cardiovascular and respiratory parameters. All testing was performed in a quiet laboratory, at normal room temperature, and at sea-level atmospheric pressure.

In the nonsmoking group, session 2 was performed to assess the reaction and recovery times of arterioles and session 3 was to ascertain if regional differences in retinal vascular reactivity existed. Therefore, the experimental protocol was slightly different for sessions 2 (protocol A) and 3 (protocol B).

- *Protocol A:* The test protocol was divided into three consecutive phases in which the subject breathed (1) room air for ~20 min, (2) 100% oxygen for ~15 to 20 min via the nonrebreather mask, and (3) room air for ~15 min. These phases were considered baseline, oxygen breathing, and recovery phases, respectively. 2 deg FOV image sequences of a suitable arteriolar segment were obtained every 30 to 60 s during this session.
- *Protocol B*: The test protocol was divided into two consecutive phases in which the subject breathed (1) room air for ~20 min and (2) 100% oxygen for ~20 min. These phases were considered baseline and oxygen breathing, respectively. A suitable arteriole was selected in each quadrant, one of them being the arteriole imaged in session 2. Approximately six 2 deg FOV image sequences of each of the arterioles were obtained at baseline. Subjects breathed oxygen for 5 min before imaging recommenced as they continued to breathe oxygen. The same arterioles imaged at baseline were reimaged and approximately six image sequences were captured.

In the smoking group, protocol A was used for both sessions 2 and 3. Session 2 was performed to assess the long-term effect of smoking on the magnitude of constriction of arterioles in response to hyperoxia and session 3 was performed to investigate the acute effect of smoking on the reactivity response. For session 2, the experimental protocol was performed after a 12-h abstinence from cigarette smoking. Volunteers also refrained from smoking for 12 h before session 3; however, they were asked to smoke a single cigarette just before the start of the experiment. The test protocol was otherwise identical for both sessions for the smokers. To assess the effect of smoking on the parameters measured, data were compared to the data obtained for the nonsmokers. As there was no significant difference between any parameters obtained for nonsmokers between sessions 2 and 3, the nonsmokers' data were averaged across both sessions when being compared to the smokers' data.

To assess the relationship between the magnitude of the reactivity response to hyperoxia and vessel caliber, data from image sequences from the nonsmoking group, which contained both a large and small arteriole, were collated. Arterioles with diameters >30 pixels (~60 μm) were categorized as large, while those with diameters <30 pixels were classed as small.

Blood pressure was measured during sessions 2 and 3. Three measurements were taken during each phase. Systolic (BP_s) and diastolic blood pressures (BP_d) were measured on the upper arm by an automated oscillometric device (Omron M10-IT; Omron Healthcare Europe BV; Hoofddorp, The Netherlands). Mean brachial artery blood pressure (BP_m) was calculated by $BP_m = BP_d + (1/3)(BP_s - BP_d)$. Pulse rate (PR) and oxygen saturation (SpO_2) were also recorded during both reactivity measurement sessions. Three readings were taken during each phase from a finger pulse oximetric device (Ohmeda Biox 3700e; Datex-Ohmeda Inc., Madison, Wisconsin). All measurements were made by the same investigator.

Diameter measurements were not converted from pixels to micrometers using axial length measurements because relative change was the primary outcome measure desired. However, for the 2 deg FOV, 1 pixel is approximately equal to 2 μm.

A change in IOP causes a change in retinal perfusion pressure. Previous studies have measured IOP at baseline and during oxygen breathing and found that IOP does not change significantly during hyperoxia.[18,34–36] Previous studies have also investigated the effect of cigarette smoking on IOP. IOP was measured before and after cigarette smoking and it was found to be unaltered by acute smoking.[20,21,37–39] It has also been

established that there is no difference in IOP values between smokers and nonsmokers.[9,22,38] Consequently, IOP was not recorded during our experiments.

Previous studies have demonstrated that the magnitude of retinal arteriolar reactivity is independent of gender[7,14,22,34] and left/right eye;[7,22] we, therefore, did not investigate reactivity as a function of these parameters.

3.3 *Data Analysis*

Statistical analysis was performed using Minitab® software package (Release 16; Minitab Inc., State College, Pennsylvania). Each dataset was group-averaged across subjects as a function of phase (i.e., baseline, hyperoxia, recovery). The response of arteriole diameters to hyperoxia is expressed as a percentage change as compared to baseline. Datasets were assessed to determine if they were normally distributed using the Anderson-Darling test. To investigate the influence of oxygen breathing on parameters, two-tailed paired t tests were performed between baseline values and hyperoxic values. To compare the effect of hyperoxia between two different groups (e.g., nonsmokers versus smokers, or large versus small arterioles), a two-tailed independent samples t test was used. A comparison of more than two groups (e.g., comparing across retinal quadrants) was performed using one-way analysis of variance (ANOVA). Variability of measurements was assessed by calculating the standard error and by comparing the results obtained between sessions 2 and 3 in the nonsmoking group. All data are presented as mean ± standard error (SE). The level of significance was set to $p < 0.05$.

4 Results

4.1 *Young, Healthy Nonsmokers*

The group-averaged values for each systemic variable for each phase of session 2 are presented in Table 1, and the values obtained for each phase of session 3 are presented in Table 2.

The results from session 2 provided us with diameter measurements throughout the experiment, allowing us to plot the diameter changes during the different phases of the experiment. The time course of the response of an arteriole diameter of a single, typical participant to a hyperoxic provocation as a function of time is shown in Fig. 6. It can be seen that vasoconstriction occurred during the first 5 min of oxygen breathing; thereafter, the diameter remained stable for the remaining 15 min of oxygen breathing. Upon cessation of the hyperoxic phase, the arteriolar diameter began to increase back to baseline. It is apparent from the plot that the reaction of the arteriole diameter to the hyperoxic stimulus is faster than the recovery back to baseline. After ~15 min of breathing room air, at the end of the oxygen breathing phase, the arteriole had returned to its prehyperoxia testing diameter. The group mean retinal arteriole diameter was 39.6 ± 1.5 pixels at baseline. This decreased significantly to 36.5 ± 1.3 pixels during oxygen breathing ($p = 0.001$) and recovered to 39.1 ± 1.6 pixels during the recovery phase of room-air breathing. The group mean percentage change in arteriolar diameter during hyperoxic provocation was −9.7 ± 1.0%.

Figure 7(a) presents a comparison of the group mean, baseline arteriolar diameters in the superior temporal (ST), inferior temporal (IT), superior nasal (SN), and inferior nasal (IN) retinal quadrants. Table 3 details the group-averaged arteriole diameter values across quadrants and hemiretinae (i.e., temporal, nasal, superior, inferior). It is apparent that the temporal arterioles are larger than the nasal arterioles ($p = 0.008$), while superior arterioles do not differ from inferior arterioles ($p = 0.725$). It is also evident that significant vasoconstriction occurred in all retinal regions. Figure 7(b) presents a comparison of the group-averaged percentage change in the arteriole diameters, relative to baseline, across the retinal quadrants during hyperoxia. Table 4 details the percentage change in diameter obtained for each retinal region. The data indicate that systemic hyperoxia induced a group-averaged arteriole constriction of −9.2 ± 0.9% (ST), −9.0 ± 0.9% (IT), −11.0 ± 1.2% (SN), and −10.6 ± 0.9% (IN). The degree of constriction does not vary across the quadrants ($p = 0.372$,

Table 2 Systemic hemodynamics obtained throughout session 3. Data are presented as mean ± SE. t tests were not performed on SpO_2 data as they were not found to be normally distributed.

Parameter ($n = 18$)	Baseline	Hyperoxia	p value (hyperoxia versus baseline)
SpO_2 (%)	97.8 ± 0.3	99.8 ± 0.1	—
PR (bpm)	73.9 ± 2.4	70.7 ± 2.0	0.002
BP_s (mm Hg)	108.0 ± 3.5	107.6 ± 3.0	0.692
BP_d (mm Hg)	62.8 ± 1.2	66.1 ± 1.6	0.001
BP_m (mm Hg)	77.9 ± 1.7	79.9 ± 1.8	0.010

Table 1 Systemic hemodynamics obtained throughout session 2. Data are presented as mean ± SE. t tests were not performed on SpO_2 data as they were not found to be normally distributed.

Parameter ($n = 16$)	Baseline	Hyperoxia	p value (hyperoxia versus baseline)	Recovery (recovery versus baseline)	p value
SpO_2 (%)	97.4 ± 0.3	99.6 ± 0.2	—	97.8 ± 0.3	—
PR (bpm)	75.0 ± 2.9	70.7 ± 2.4	0.011	74.5 ± 2.7	0.763
BP_s (mm Hg)	107.4 ± 3.7	107.4 ± 3.7	0.934	108.6 ± 3.4	0.529
BP_d (mm Hg)	64.0 ± 2.2	65.0 ± 1.9	0.302	66.4 ± 2.0	0.152
BP_m (mm Hg)	78.5 ± 2.5	79.1 ± 2.2	0.377	80.1 ± 2.3	0.352

PR, pulse rate; BP_s, systolic blood pressure; BP_d, diastolic blood pressure; BP_m, mean brachial artery blood pressure.

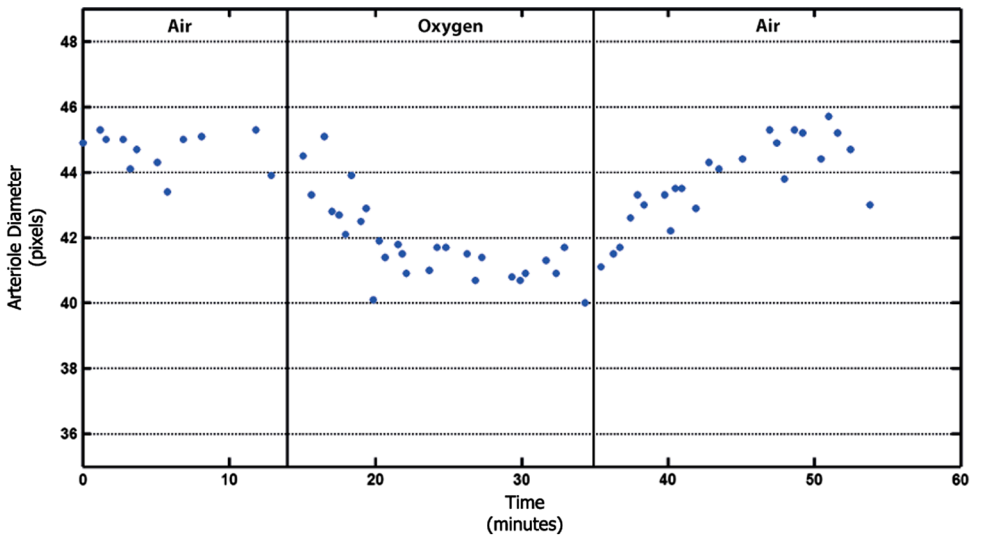

Fig. 6 Change in the retinal arteriole diameter of a single, typical participant induced by hyperoxia as a function of time. Vertical lines represent the points at which oxygen breathing started and stopped. A pixel subtends ~2 μm. The arteriole diameter decreases during the first 5 min of oxygen breathing, plateaus, and remains stable for the rest of the oxygen breathing phase. The arteriole diameter increases during the air breathing, recovery phase and has returned to baseline after ~15 min.

ANOVA). A comparison of the magnitude of arteriolar constriction in the hemiretinal regions, i.e., temporal versus nasal and superior versus inferior, revealed that the arterioles in the temporal retina appeared to constrict slightly less than those nasally, but this was not significant ($p = 0.080$), and the arterioles in the superior retina responded to the same degree as those in the inferior retina ($p = 0.725$).

The group mean baseline diameter for the narrow arteriolar measurement site was 19.2 ± 0.8 pixels (~38.4 ± 1.6 μm) ($n = 18$), and for the wide measurement site, it was 36.1 ± 0.7 pixels (72.2 ± 1.4 μm) ($n = 22$). The group mean diameter constriction of the small arterioles was -1.9 ± 0.2 pixels and for the large arterioles, it was -3.4 ± 0.2 pixels. There was a significant difference in the absolute change in diameter between large and small arterioles ($p = 0.000$). The group-averaged percentage change in diameter of the small arterioles was $-9.8 \pm 0.8\%$ and for large arterioles, it was $-9.2 \pm 0.6\%$. There was no difference in the percentage constriction between the large and small vessels ($p = 0.538$).

The arteriole imaged during session 2, to study the reaction and recovery time, was also chosen as one of the four vessels imaged in session 3, to study regional differences in reactivity. To assess the repeatability of our measurements, the values obtained for these arterioles during the two sessions are

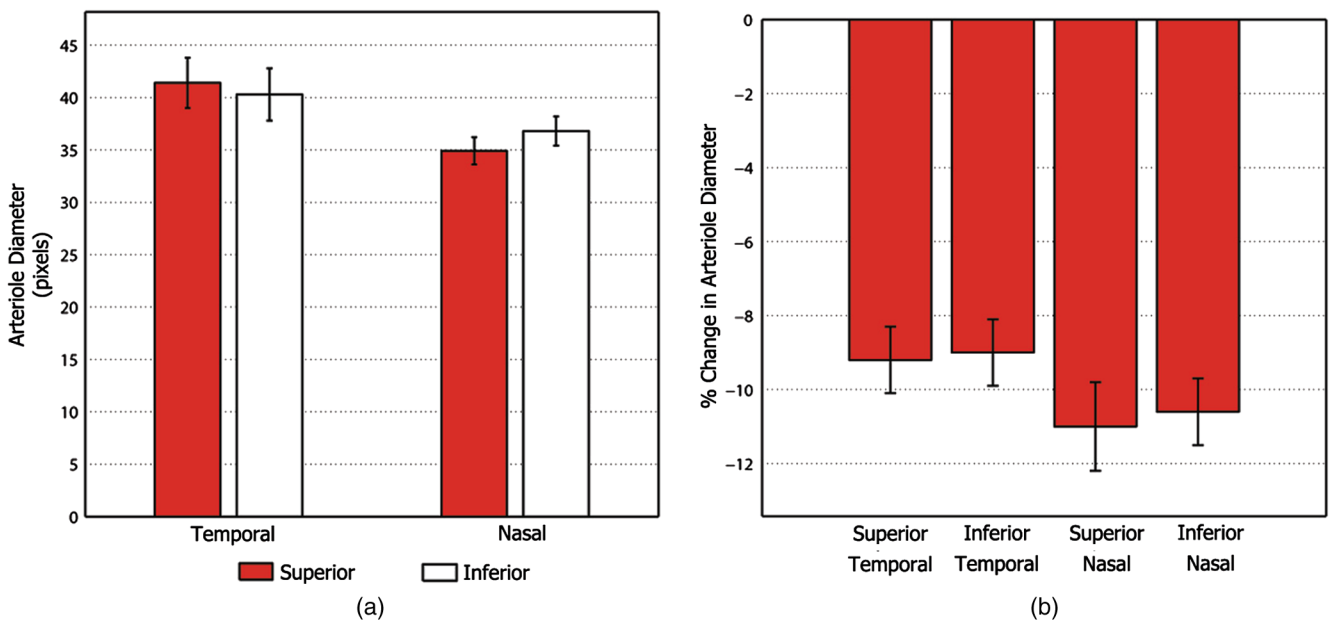

Fig. 7 (a) Baseline, group mean arteriole diameters in the retinal quadrants. A pixel subtends ~2 μm. (b) Comparison of the percentage change in arteriolar diameter from baseline, across retinal quadrants. Data are presented as mean ± SE.

Table 3 Comparing arteriole diameters across retinal regions, before and during hyperoxic provocation. Data are presented as mean ± SE.

Retinal region	Baseline diameter (pixels)	Hyperoxic diameter (pixels)	*p* value (hyperoxic versus baseline)
ST ($n = 14$)	41.4 ± 2.4	37.5 ± 2.3	0.000
IT ($n = 16$)	40.3 ± 2.5	36.6 ± 2.1	0.000
SN ($n = 16$)	34.9 ± 1.3	31.0 ± 1.1	0.000
IN ($n = 16$)	36.8 ± 1.4	32.8 ± 1.2	0.000
Temporal ($n = 30$)	40.9 ± 1.7	37.0 ± 1.5	0.000
Nasal ($n = 32$)	35.8 ± 0.9	31.9 ± 0.8	0.000
Superior ($n = 30$)	38.2 ± 1.4	34.0 ± 1.3	0.000
Inferior ($n = 32$)	38.3 ± 1.4	34.7 ± 1.2	0.000

ST, superior temporal; IT, inferior temporal; SN, superior nasal; IN, inferior nasal.

Table 4 Comparing the percentage difference of arteriole diameters due to hyperoxia, compared to baseline, across retinal regions. Data are presented as mean ± SE.

Retinal region	% difference
ST ($n = 14$)	−9.2 ± 0.9
IT ($n = 16$)	−9.0 ± 0.9
SN ($n = 16$)	−11.0 ± 1.2
IN ($n = 16$)	−10.6 ± 0.9
Temporal ($n = 30$)	−9.1 ± 0.6
Nasal ($n = 32$)	−10.8 ± 0.7
Superior ($n = 30$)	−10.1 ± 0.8
Inferior ($n = 32$)	−9.8 ± 0.6

compared. The group mean baseline diameter of the arterioles in session 2 was 38.1 ± 2.1 pixels and in session 3, it was found to be 39.1 ± 1.9 pixels. There was no difference in the baseline diameters between visits ($p = 0.907$). During the hyperoxic phase of session 2, the arterioles decreased to 35.2 ± 1.9 pixels, and in session 3, they decreased to 35.6 ± 1.9 pixels. There was no difference, between the two visits, in the hyperoxic diameters measured ($p = 0.888$). The group-averaged constriction reached in session 2 was −9.3 ± 1.2% and in session 3, it was found to be −9.6 ± 1.2%. There was no difference in the magnitude of vasoconstriction between visits ($p = 0.871$), while the mean difference in the percentage change of diameter between visits was 0.3 ± 0.8% (mean ± SE).

4.2 *Young, Otherwise Healthy Smokers*

The group-averaged values for each systemic variable for each phase of session 2 (abstinence from smoking for 12 h, $\text{smokers}_{[\text{no cig}]}$) are presented in Table 5, and the values obtained for each phase of session 3 (cigarette smoked immediately before commencement of experiment, $\text{smokers}_{[\text{post cig}]}$) are presented in Table 6.

Table 7 details the group-averaged arteriole diameter values across groups (i.e., $\text{smokers}_{[\text{no cig}]}$, $\text{smokers}_{[\text{post cig}]}$, and nonsmokers). Figure 8(a) presents a comparison of the group mean, baseline arteriolar diameters in $\text{smokers}_{[\text{no cig}]}$, $\text{smokers}_{[\text{post cig}]}$, and nonsmokers. It is evident from this plot that the baseline diameters did not differ between $\text{smokers}_{[\text{no cig}]}$ and $\text{smokers}_{[\text{post cig}]}$. Although the baseline group mean arteriole diameters of the nonsmoking group appear to be a little larger than those of the smoking group, we did not find a significant difference between the groups ($p = 0.186$). It is also apparent from the data in Table 7 that significant vasoconstriction occurred in all three groups.

Table 8 details the percentage change in diameter obtained for each group. Figure 8(b) presents a comparison of the group-averaged percentage change in the arteriole diameters, relative to baseline, attained by $\text{smokers}_{[\text{no cig}]}$, $\text{smokers}_{[\text{post cig}]}$, and nonsmokers, during the hyperoxic phase. The data indicate that the degree of vasoconstriction achieved by the smokers was the same when measured after a 12-h abstinence and immediately after smoking a cigarette ($p = 0.621$). The reactivity of smokers was, however, significantly less than that of nonsmokers ($\text{smokers}_{[\text{no cig}]}$ versus nonsmokers, $p = 0.017$; $\text{smokers}_{[\text{post cig}]}$ versus nonsmokers, $p = 0.004$). In the recovery

Table 5 Systemic hemodynamics obtained throughout session 2 (no cigarette). Data are presented as mean ± SE. *t* tests were not performed on SpO_2 data as they were not found to be normally distributed.

Parameter ($n = 12$)	Baseline	Hyperoxia	*p* value (hyperoxia versus baseline)	Recovery	*p* value (recovery versus baseline)
SpO_2 (%)	97.7 ± 0.3	99.6 ± 0.2	—	97.4 ± 0.4	—
PR (bpm)	72.5 ± 3.0	70.1 ± 2.1	0.252	70.3 ± 2.5	0.131
BP_s (mm Hg)	113.8 ± 3.7	109.7 ± 2.3	0.104	108.5 ± 2.3	0.013
BP_d (mm Hg)	69.9 ± 2.1	66.8 ± 1.3	0.043	68.5 ± 1.6	0.351
BP_m (mm Hg)	84.5 ± 2.5	81.1 ± 1.6	0.030	82.5 ± 1.6	0.267

Table 6 Systemic hemodynamics obtained throughout session 3 (post cigarette). Data are presented as mean ± SE. *t* tests were not performed on SpO_2 data as they were not found to be normally distributed.

Parameter ($n = 12$)	Baseline	Hyperoxia	*p* value (hyperoxia versus baseline)	Recovery	*p* value (recovery versus baseline)
SpO_2 (%)	97.7 ± 0.5	99.5 ± 0.2	—	97.4 ± 0.5	—
PR (bpm)	86.3 ± 4.4	78.2 ± 3.3	0.001	79.9 ± 2.0	0.009
BP_s (mm Hg)	118.1 ± 2.0	112.6 ± 2.1	0.001	113.5 ± 2.6	0.016
BP_d (mm Hg)	70.5 ± 1.5	67.7 ± 1.2	0.016	67.8 ± 1.7	0.027
BP_m (mm Hg)	86.4 ± 1.5	82.7 ± 1.2	0.001	83.1 ± 1.8	0.003

Table 7 Comparing arteriole diameters for each experimental phase (i.e., baseline, hyperoxia, and recovery) by smoking status. Data are presented as mean ± SE.

	Baseline diameter (pixels)	Hyperoxic diameter (pixels)	*p* value (hyperoxia versus baseline)	Recovery diameter (pixels)	*p* value (recovery versus baseline)
$Smokers_{[no\ cig]}$ ($n = 17$)	35.3 ± 2.6	32.8 ± 2.5	0.000	35.5 ± 2.7	0.498
$Smokers_{[post\ cig]}$ ($n = 17$)	35.2 ± 2.6	32.8 ± 2.5	0.000	35.4 ± 2.7	0.328
Nonsmokers	38.5 ± 0.8 ($n = 82$)	34.8 ± 0.8 ($n = 78$)	0.001	39.1 ± 1.6 ($n = 16$)	0.766

phase, the arteriolar diameters of each group returned to their prehyperoxic diameters.

The time course of the response of an arteriole diameter of a single, typical smoker to hyperoxic provocation as a function of time is portrayed in Fig. 9. The red dots represent the response of the arteriole diameter to hyperoxia after a 12-h abstinence from smoking. The black crosses describe the response of the diameter of the same arteriole segment to hyperoxia immediately after smoking a cigarette. The vertical lines in the plot mark the points at which oxygen breathing started and stopped.

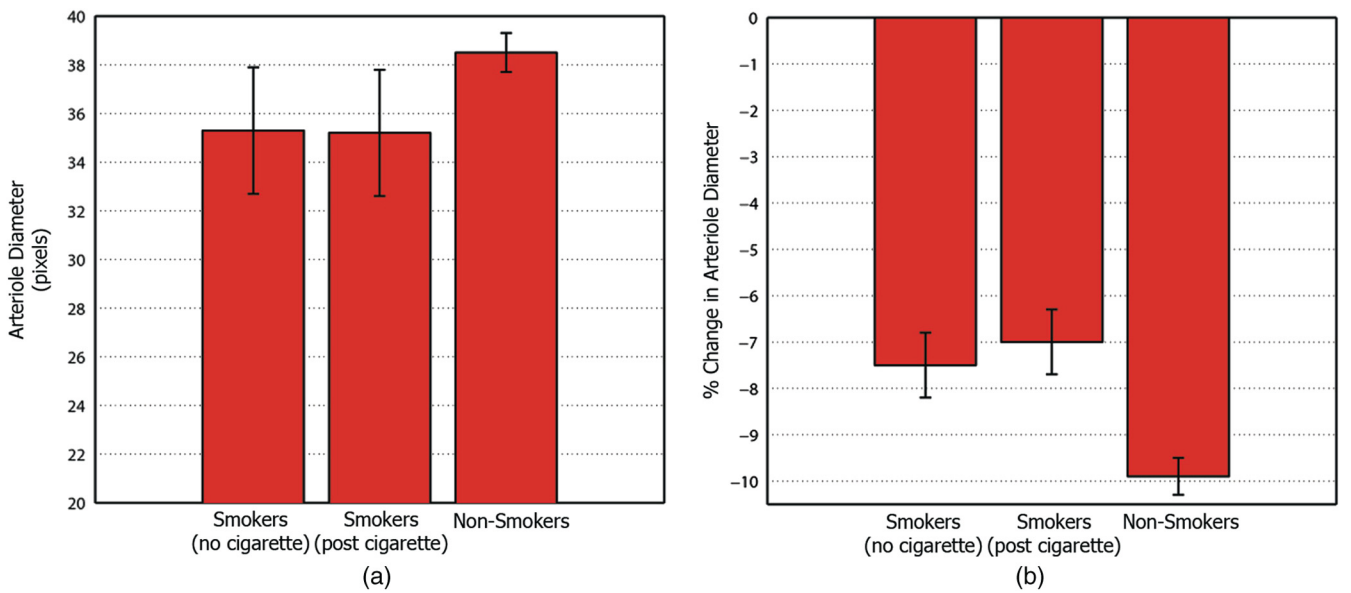

Fig. 8 (a) Baseline, group mean arteriolar diameters in the retinal quadrants. A pixel subtends ~2 μm. (b) Comparison of the percentage change in arteriolar diameter from baseline, across retinal quadrants. Data are presented as mean ± SE.

Table 8 Comparing the percentage difference in arteriole diameters due to hyperoxia, compared to baseline, across smoking status. Data are presented as mean ± SE.

	% difference
$\text{Smokers}_{[\text{no cig}]}$ ($n = 17$)	−7.5 ± 0.7
$\text{Smokers}_{[\text{post cig}]}$ ($n = 17$)	−7.0 ± 0.7
Nonsmokers ($n = 78$)	−9.9 ± 0.4

It is evident that smoking a cigarette had no effect on the response of the arteriole diameter to hyperoxia.

5 Discussion

The increased level of SpO_2 during the oxygen breathing phase of all the experiments suggests that systemic hyperoxia was achieved. The pulse rate of the smokers increased significantly after smoking a cigarette, indicating that substantial levels of nicotine were absorbed. Some changes in PR and BP were observed in subjects during the experiments. The magnitude of these changes, however, was small and would not be expected to influence the degree of vasoconstriction measured. For example, the largest changes in PR and BP_m recorded in our subjects were 8.1 bpm and 3.7 mm Hg, while studies that used isometric exercise to cause vasoconstriction[4–6] reported that very large changes in BP (16.7 to 33.4 mm Hg) and heart rate [30 bpm (Ref. 6)] elicited relatively small vasoconstrictions of 0.2 to 3.4%.

The results from the nonsmoking group indicate that vasoconstriction occurs during the first 5 min of oxygen breathing, after which time the arterioles are maximally constricted and remain stable for the remainder of the oxygen breathing phase. The rate of vasoconstriction was found to be greater than the rate of recovery. Arteriole diameters had recovered to their prehyperoxia baseline values after ~15 min of breathing room air in the recovery phase. Our results are in line with previously published data.[14–16,35] As vasoconstriction was complete 5 min after oxygen breathing commenced, this was set as the standard time subjects breathed oxygen before measurements for the hyperoxic phase commenced for the subsequent experiments in session 3 with the nonsmokers. The group mean percentage change in arteriolar diameter during hyperoxic provocation was −9.7 ± 1.0%. This result compares well with those in other studies that used 100% oxygen to investigate retinal arteriolar reactivity. In these studies, investigators recorded reductions of arteriole diameters of −9.2,[14] −12.0,[15] −15.0,[16] −7.8,[17] −11.5,[34] −12.1,[35] −8.7,[40] and −9.0%.[41]

Previously published data have consistently reported that blood flow,[42–44] velocity,[42] and vessel diameter[14,42] are greater in the temporal retina versus the nasal retina. These parameters, however, do not differ when comparing the superior retina to the inferior retina.[14,34,43,44] Our results indicate that temporal arteriolar diameters are larger than those in the nasal retina, while they do not differ between the superior and inferior retina. Therefore, we can conclude that our results are in agreement with previous findings. It has been hypothesized that blood flow is greater to the temporal hemiretina as it is 20 to 25% larger than the nasal hemiretina[13,42] and it contains the highly metabolic macula.[14,42]

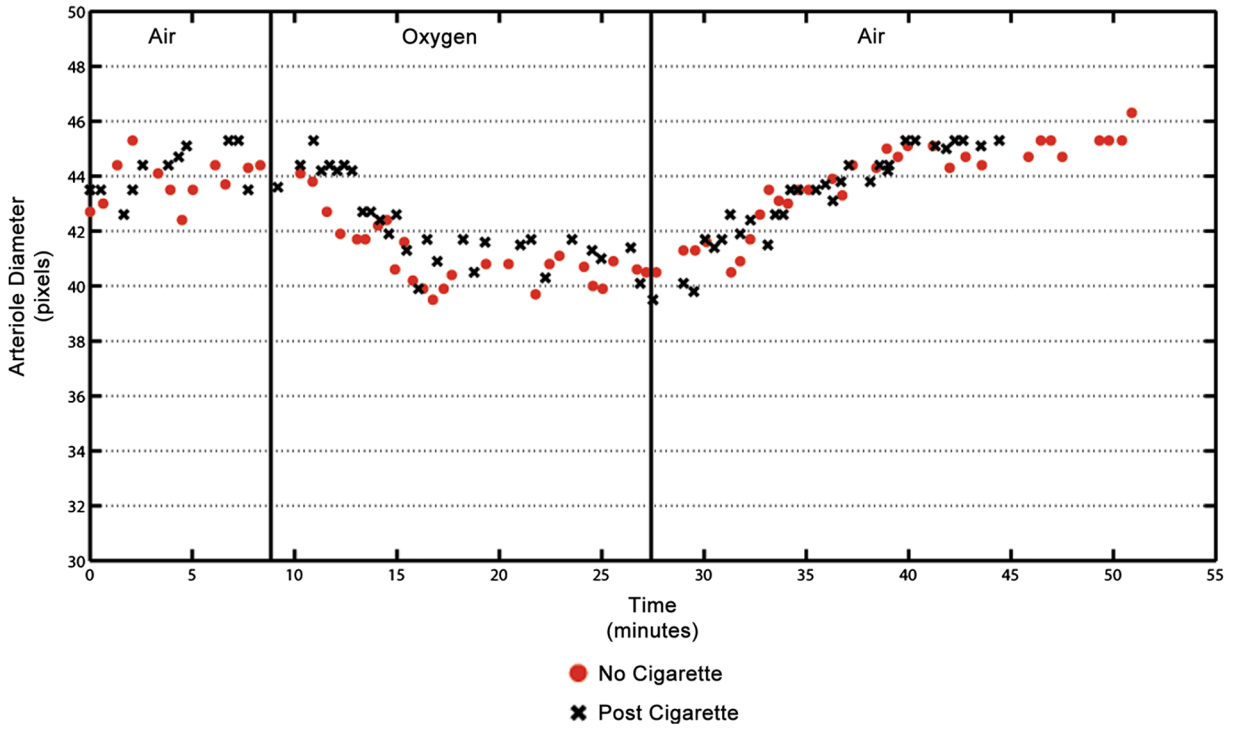

Fig. 9 Change in the retinal arteriole diameter of a single, typical smoker, induced by hyperoxia as a function of time. The red dots depict the response to the arteriole diameter to hyperoxia after a 12-h abstinence from smoking. The black crosses delineate the arteriolar diameter response immediately after smoking a cigarette. The vertical lines mark the points at which oxygen breathing started and stopped. There is no difference in the arteriolar response to hyperoxia between sessions.

To our knowledge, only a handful of studies have investigated whether regional variations in the degree of reactivity exist;[14,15,34,42,45] the results of these studies have not been entirely decisive. Our results indicated that there was no difference in the percentage change across the quadrants. When comparing the hemiretinal areas (i.e., temporal versus nasal and superior versus inferior), again, no significant difference in vasoconstriction was found. Three of the previous studies found no difference across regions,[14,34,42] while two studies found a difference in reactivity in different regions.[15,45] Our results are in agreement with the majority of the small number of studies in this area.[14,34,42] Therefore, while it has been postulated that a differential autoregulatory response may exist between the temporal and nasal regions, the results lead us to conclude that the reactivity response is independent of retinal region.

It is well known that smaller (resistance) arteries demonstrate a much greater ability to modulate diameter in order to regulate blood flow in response to a change in BP or an alteration of the metabolic needs of a tissue than large (conducting) arteries.[1,46,47] Some studies have reported results that suggest that even within the relatively small range of vessel diameters present in the retina, a dependency exists between the magnitude of reactivity of a vessel and its initial caliber. Two previous studies observed an inverse relationship between the arteriole diameter and the percentage diameter response.[5,15] Our study found that the absolute change in diameter was greater for large than for small arterioles, while the percentage difference from baseline was the same between vessels of different caliber. A number of other studies also found that the percentage change in vessel diameter from the baseline due to a stimulus was not dependent on vessel size.[3,7,11,12,23] At the level of the retina, all arteries have an arteriolar structure,[13] so it is of little surprise that our observations are in line with the majority of retinal studies comparing the magnitude of reactivity between large and small vessels. We, therefore, conclude that the magnitude of the percentage change in retinal arterioles is independent of baseline arteriole diameter.

As the degree of vasoconstriction was independent of retinal region and vessel size, a reactivity measurement taken from a single, arbitrary site can be considered as representative of the reactivity response of the retinal vasculature as a whole.

The baseline and hyperoxic diameters and the percentage constriction obtained for the arterioles were found not to differ between sessions 2 and 3. Also, the mean difference in the percentage change of diameters between visits was $0.3 \pm 0.8\%$ (mean $\pm$ SE). This suggests that this method of measuring retinal arteriolar diameters and the change in diameter in response to a stimulus has a high reproducibility.

The baseline arteriolar results obtained from smokers$_{[\text{no cig}]}$ suggest that their baseline arteriolar diameters did not differ from those of the nonsmoking group. This result is in agreement with the bulk of previous studies, which found that retinal vessel diameter, blood flow velocity, and blood flow of the retina, optic nerve head, and choroid did not differ between smokers$_{[\text{no cig}]}$ and nonsmokers at baseline.[9,22,38,48–50] Only Wimpissinger et al.[48] found a difference between the groups, reporting higher choroidal blood flow in smokers compared to nonsmokers. Our results comparing baseline diameters of smokers to nonsmokers do need to be treated with a degree of caution, however, as we did not convert our diameter measurements into absolute units, making them ill-suited for interindividual comparisons. This limitation, however, does not apply when comparing the baseline diameters of smokers$_{[\text{no cig}]}$ and smokers$_{[\text{post cig}]}$. We are somewhat hesitant to draw conclusions from an intergroup comparison of diameter, however, as our results are in line with previous findings, we believe it is reasonable to conclude that baseline diameters of smokers$_{[\text{no cig}]}$ do not differ from those of nonsmokers.

The results of the acute effects of cigarette smoking on blood flow in the retina have been somewhat more controversial. We found that arteriolar diameter was unchanged after smoking. We found five papers that used an retinal vessel analyzer (RVA),[37] the laser speckle method,[20,21] the blue field entoptic phenomenon,[51] and retinal photography[39] to report on the acute effects of smoking on retinal blood flow. Two found no change in flow after smoking,[21,37] one found a small decrease,[39] and two found an increase.[20,51] From the existing evidence, we believe that retinal arteriolar diameter is unaffected by acute smoking.

Previous studies of the effect of chronic smoking on the reactivity response to various stimuli used various measurement techniques: an RVA,[9,48,50] laser Doppler velocimetry,[9,50] laser Doppler flowmetry,[38] and scanning laser Doppler flowmetry.[49] They were inconsistent with regard to their findings. Two studies observed a reduced reactivity response in smokers$_{[\text{no cig}]}$ when compared to nonsmokers,[9,49] two studies observed an increased response,[38,50] and one study recorded no difference.[48] We found the reactivity response of smokers$_{[\text{no cig}]}$ to be decreased when compared to nonsmokers. In smokers, endothelium-dependent reactivity has been shown to be impaired in many other vascular beds,[52–58] which is in agreement with our results. Based on the available data, it seems likely that retinal vascular function is impaired due to chronic smoking, but further work is required to confirm this.

In agreement with our findings for the effect of acute smoking on the reactivity response, Cubbidge et al.[37] and Morgado et al.[39] found no difference in the magnitude of arteriolar constriction when comparing smokers after abstinence and after smoking a cigarette. As our results confirm those of both previous studies, we conclude that endothelium-dependent reactivity in the retinal vasculature is unaltered by acute smoking.

What is the cause of this reduced reactivity response due to chronic smoking? It is widely reported that cigarette smoking is associated with reduced levels of nitric oxide.[1,56,59–61] Some studies have also found increased levels of endothelin-1.[50,59] Our results do not necessarily fit with these observations. Reduced nitric oxide (NO) availability or increased endothelin-1 (ET-1) would result in vasoconstriction. We did not find the baseline arteriolar diameters of smokers$_{[\text{no cig}]}$ to be decreased compared to nonsmokers and baseline diameters were not reduced in smokers after cigarette smoking. This does not indicate an alteration in the levels of endothelium-secreted vasoactive factors. With the relatively small number of subjects measured in this study and the high interindividual scatter associated with diameter measurements, it is possible that large numbers of subjects are required for a significant difference to be established. We cannot offer a ready explanation for the discrepancy based on the data available in this study, and, therefore, further work is necessary. Previous studies have used endothelium-independent vasodilators (e.g., glyceryl trinitrate and nitroglycerin) to establish that endothelium-independent arteriolar dilation was unimpaired[53,55,56,58,62,63] in smokers. This implies that the blunted endothelium-dependent responses are due to endothelial dysfunction and not due to degeneration of the vascular smooth muscle cells.[56,63] We can, therefore, conclude that the blunted vasoconstriction

observed in the smokers in our study was indeed due to endothelial dysfunction, but the precise nature of this dysfunction has yet to be elucidated.

A possible source error in our experiments is that some subjects may have failed to abstain from smoking before the experiments. The importance of abstinence was explained to the volunteers, so it is believed that if some subjects did smoke during the abstinence period, it would have been a very small number that would have done so.

If reactivity measurements are to be used to facilitate early diagnosis, risk prediction, or treatment monitoring in disease, it is necessary to know how factors such as smoking affect the parameter. We found that chronic smoking blunts the reaction of arterioles to a stimulus; however, it is not known if this is reversed after quitting and if it is, the timeline of this reversal needs to be elucidated. It is also unknown if vascular reactivity continues to decrease as the number of years of smoking or the number of cigarettes smoked per day increases. A greater understanding of the effects of smoking on endothelial function is required.

6 Conclusion

We measured the reactivity responses of young, healthy smokers and nonsmokers to a high degree of accuracy using a high-resolution SLO and image processing techniques. To our knowledge, this is the first time a high-resolution imaging technique has been applied to the task of measuring diameter changes to assess vascular reactivity. This allowed us to measure the reactivity response in retinal arterioles of smaller caliber ($\sim$40 μm) than previous studies, which assessed vessels measuring $\geq$80 μm. Our results showed good agreement with the literature data for established results, which verifies the validity of our measurements. For example, we observed that the retinal arterioles constricted during the first 5 min of oxygen breathing, after which they were maximally constricted and diameters remained stable for the remainder of the oxygen breathing phase. The reaction of arteriole diameters to hyperoxia was faster than their recovery to baseline. The group mean percentage change in arteriolar diameter in nonsmokers was $-9.7 \pm 1.0\%$. Blood flow to the temporal retina was higher than to the nasal retina, while flow to the superior and inferior retinae did not differ. All of these results are congruent with the consistent findings of previous studies. We also added valuable data to more controversial areas. We determined that retinal arteriolar diameters are unchanged by acute cigarette smoking. Our results indicate that the retinal arteriolar response to hyperoxia is blunted in smokers compared to nonsmokers, suggesting impaired endothelial function from long-term smoking, while acute smoking had no effect on the magnitude of hyperoxia-induced vasoconstriction. Therefore, the application of a high-resolution imaging system to the procurement of more accurate vessel diameter measurements in blood flow regulation studies offers a high potential to resolve previous equivocal results and may afford greater insight in future studies of pathology.

Acknowledgments

This research was supported by the National Biophotonics and Imaging Platform, Ireland, and funded by the Irish Government's Programme for Research in Third Level Institutions, Cycle 4, National Development Plan 2007 to 2013, and through Science Foundation Ireland under Grant No. SFI/07/IN.1/1906. J.C.D. is supported by the NIHR Moorfields Biomedical Research Centre.

References

1. J. R. Levick, *An Introduction to Cardiovascular Physiology*, 5th ed., Hodder Arnold, London, UK (2011).
2. I. O. Haefliger et al., "Endothelium-dependent vasoactive modulation in the ophthalmic circulation," *Prog. Retin. Eye Res.* **20**(2), 209–225 (2001).
3. S. T. Venkataraman et al., "Retinal arteriolar and capillary vascular reactivity in response to isoxic hypercapnia," *Exp. Eye Res.* **87**, 535–542 (2008).
4. M. J. Dumskyj et al., "Autoregulation in the human retinal circulation: assessment using isometric exercise, laser Doppler velocimetry, and computer-assisted image analysis," *Microvasc. Res.* **51**, 378–392 (1996).
5. P. Jeppesen, J. Sanye-Hajari, and T. Bek, "Increased blood pressure induces a diameter response of retinal arterioles that increases with decreasing arteriolar diameter," *IOVS* **48**(1), 328–331 (2007).
6. F. Robinson et al., "Retinal blood flow autoregulation in response to an acute increase in blood pressure," *IOVS* **27**(5), 722–726 (1986).
7. H. Tachibana, F. Gotoh, and Y. Ishikawa, "Retinal vascular autoregulation in normal subjects," *Stroke* **13**(2), 149–155 (1982).
8. C. E. Riva, J. E. Grunwald, and B. L. Petrig, "Autoregulation of human retinal blood flow. An investigation with laser Doppler velocimetry," *IOVS* **27**(12), 1706–1712 (1986).
9. G. Garhöfer et al., "Effect of regular smoking on flicker induced retinal vasodilatation in healthy subjects," *Microvasc. Res.* **82**(3), 351–355 (2011).
10. R. Heitmar and R. J. Summers, "Assessing vascular function using dynamic retinal diameter measurements: a new insight on the endothelium," *Thromb. Haemost.* **107**, 1019–1026 (2012).
11. E. Nagel, W. Vilser, and I. Lanzl, "Age, blood pressure, and vessel diameter as factors influencing the arterial retinal flicker response," *IOVS* **45**(5), 1486–1492 (2004).
12. K. Polak, L. Schmetterer, and C. E. Riva, "Influence of flicker frequency on flicker-induced changes of retinal vessel diameter," *IOVS* **43**(8), 2721–2726 (2002).
13. C. J. Pournaras et al., "Regulation of retinal blood flow in health and disease," *Prog. Retin. Eye Res.* **27**, 284–330 (2008).
14. S. Jean-Louis, J. V. Lovasik, and H. Kergoat, "Systemic hyperoxia and retinal vasomotor responses," *IOVS* **46**(5), 1714–1720 (2005).
15. B. Kiss et al., "Retinal blood flow during hyperoxia in humans revisited: concerted results using different measurement techniques," *Microvasc. Res.* **64**(1), 75–85 (2002).
16. A. Luksch et al., "Effect of inhalation of different mixtures of O2 and CO2 on retinal blood flow," *Br. J. Ophthalmol.* **86**(10), 1143–1147 (2002).
17. B. L. Justesen et al., "Retinal arterioles have impaired reactivity to hyperoxia in type 1 diabetes," *Acta Ophthalmol.* **88**(4), 453–457 (2010).
18. S. J. Pakola and J. E. Grunwald, "Effects of oxygen and carbon dioxide on human retinal circulation," *IOVS* **34**(10), 2866–2870 (1993).
19. W. E. Sponsel, K. L. DePaul, and S. R. Zetlan, "Retinal hemodynamic effects of carbon dioxide, hyperoxia, and mild hypoxia," *IOVS* **33**(6), 1864–1869 (1992).
20. Y. Tamaki et al., "Acute effects of cigarette smoking on tissue circulation in human optic nerve head and choroid-retina," *Ophthalmology* **106**(3), 564–569 (1999).
21. Y. Tamaki et al., "The acute effects of cigarette smoking on human optic nerve head and posterior fundus circulation in light smokers," *Eye* **14**(1), 67–72 (2000).
22. R. Heitmar et al., "Continuous retinal vessel diameter measurements—the future of retinal vessel assessment?," *IOVS* **51**(11), 5833–5839 (2010).
23. F. Tayyari et al., "The relationship between retinal vascular reactivity and arteriolar diameter in response to metabolic provocation," *IOVS* **50**(10), 4814–4821 (2009).
24. S. T. Venkataraman et al., "Novel methodology to comprehensively assess retinal arteriolar vascular reactivity to hypercapnia," *Microvasc. Res.* **72**, 101–107 (2006).

25. G. Garhöfer et al., "Use of the retinal vessel analyser in ocular blood flow research," *Acta Ophthalmol.* **88**, 717–722 (2010).
26. K. Guan et al., "Retinal hemodynamics in early diabetic macular edema," *Diabetes* **55**, 813–818 (2006).
27. C. A. Girkin, "Principles of confocal scanning laser ophthalmoscopy for the clinician," http://goo.gl/WGmq88.
28. S. Stevenson and A. Roorda, "Correcting for miniature eye movements in high resolution scanning laser ophthalmoscopy," *Proc. SPIE* **5688**, 145–151 (2005).
29. A. Dubra and Z. Harvey, "Registration of 2D images from fast scanning ophthalmic instruments," *Lec. Notes Comput. Sci.* **6204**, 60–71 (2010).
30. D. W. Arathorn et al., "Retinally stabilized cone-targeted stimulus delivery," *Opt. Express* **15**, 13731–13744 (2007).
31. C. R. Vogel et al., "Retinal motion estimation in adaptive optics scanning laser ophthalmoscopy," *Opt. Express* **14**, 487–497 (2006).
32. J. P. Lewis, "Fast template matching," *Vision Interface* **10**(1), 120–123 (1995).
33. N. Chapman et al., "Computer algorithms for the automated measurement of retinal arteriolar diameters," *Br. J. Ophthalmol.* **85**(1), 74–79 (2001).
34. M. Sehi et al., "Relative magnitude of vascular reactivity in the major arterioles of the retina," *Microvasc. Res.* **83**, 200–204 (2012).
35. C. E. Riva, J. E. Grunwald, and S. H. Sinclair, "Laser Doppler velocimetry study of the effect of pure oxygen breathing on retinal blood flow," *IOVS* **24**(1), 47–51 (1983).
36. L. F. Schmetterer et al., "Topical measurement of fundus pulsations," *Opt. Eng.* **34**(3), 711–716 (1995).
37. R. Cubbidge, R. J. Summers, and R. Heitmar, "Retinal vessel reactivity after cigarette smoking," *Acta Ophthalmol.* **90**, 0–0 (2012).
38. B. Wimpissinger et al., "Effects of isometric exercise on subfoveal choroidal blood flow in smokers and nonsmokers," *IOVS* **44**(11), 4859–4863 (2003).
39. P. B. Morgado et al., "The acute effect of smoking on retinal blood flow in subjects with and without diabetes," *Ophthalmology* **101**, 1220–1226 (1994).
40. N. Chapman et al., "Acute effects of oxygen and carbon dioxide on retinal vascular network geometry in hypertensive and normotensive subjects," *Clin. Sci.* **99**, 483–488 (2000).
41. T. A. Deutsch et al., "Effects of oxygen and carbon dioxide on the retinal vasculature in humans," *Arch. Ophthalmol.* **101**(8), 1278–1280 (1983).
42. S. M. B. Rassam et al., "Regional retinal blood flow and vascular autoregulation," *Eye* **10**, 331–337 (1996).
43. G. T. Feke et al., "Blood flow in the normal human retina," *IOVS* **30**(1), 58–65 (1989).
44. C. E. Riva et al., "Blood velocity and volumetric flow rate in human retinal vessels," *IOVS* **26**(8), 1124–1132 (1985).
45. H. S. Chung et al., "Regional differences in retinal vascular reactivity," *IOVS* **40**(10), 2448–2453 (1999).
46. M. J. Mulvany and C. Aalkjaer, "Structure and function of small arteries," *Physiol. Rev.* **70**(4), 921–961 (1990).
47. C. A. Giller et al., "Cerebral arterial diameters during changes in blood pressure and carbon dioxide during craniotomy," *Neurosurgery* **32**, 737–741 (1993).
48. B. Wimpissinger et al., "Response of choroidal blood flow to carbogen breathing in smokers and non-smokers," *Br. J. Ophthalmol.* **88**(6), 776–781 (2004).
49. M. Langhans, G. Michelson, and M. J. M. Groh, " Effect of breathing 100% oxygen on retinal and optic nerve head capillary blood flow in smokers and non-smokers," *Br. J. Ophthalmol.* **81**(5), 365–369 (1997).
50. B. Wimpissinger et al., "Response of retinal blood flow to systemic hyperoxia in smokers and nonsmokers," *Graefes Arch. Clin. Exp. Ophthalmol.* **243**, 646–652 (2005).
51. F. Robinson, B. L. Petrig, and C. E. Riva, "The acute effect of cigarette smoking on macular capillary blood flow in humans," *IOVS* **26**(5), 609–613 (1985).
52. R. L. Rogers et al., "The effects of chronic cigarette smoking on cerebrovascular responsiveness to 5% CO2 and 100% O2 inhalation," *J. Am. Geriatr. Soc.* **32**(6), 415–420 (1984).
53. A. M. Zeiher, V. Schachinger, and J. Minners, "Long-term cigarette smoking impairs endothelium-dependent coronary arterial vasodilator function," *Circulation* **92**, 1094–1100 (1995).
54. D. S. Celermajer et al., "Cigarette smoking is associated with dose-related and potentially reversible impairment of endothelium-dependent dilation in healthy young adults," *Circulation* **88**(5), 2149–2155 (1993).
55. D. S. Celermajer et al., "Passive smoking and impaired endothelium-dependent arterial dilation in healthy young adults," *N. Engl. J. Med.* **334**, 150–154 (1996).
56. R. S. Barua et al., "Dysfunctional endothelial nitric oxide biosynthesis in healthy smokers with impaired endothelium-dependent vasodilatation," *Circulation* **104**, 1905–1910 (2001).
57. P. Poredos, M. Orehek, and E. Tratnik, "Smoking is associated with dose-related increase of intima-media thickness and endothelial dysfunction," *Angiology* **50**(3), 201–208 (1999).
58. R. G. Ijzerman et al., "Cigarette smoking is associated with an acute impairment of microvascular function in humans," *Clin. Sci.* **104**, 247–252 (2003).
59. M. M. Rahman and I. Laher, "Structural and functional alteration of blood vessels caused by cigarette smoking: an overview of molecular mechanisms," *Curr. Vasc. Pharmacol.* **5**, 276–292 (2007).
60. J. A. Ambrose and R. S. Barua, "The pathophysiology of cigarette smoking and cardiovascular disease: an update," *J. Am. Coll. Cardiol.* **43**(10), 1731–1737 (2004).
61. M. A. H. Talukder et al., "Chronic cigarette smoking causes hypertension, increased oxidative stress, impaired NO bioavailability, endothelial dysfunction, and cardiac remodeling in mice," *Am. J. Physiol.–Heart C.* **300**(1), 388–396 (2011).
62. J. Lekakis et al., "Effect of acute cigarette smoking on endothelium-dependent brachial artery dilation in healthy individuals," *Am. J. Cardiol.* **79**, 529–531 (1997).
63. G. E. McVeigh et al., "Effects of long-term cigarette smoking on endothelium-dependent responses in humans," *Am. J. Cardiol.* **78**, 668–672 (1996).

Margaret O' Halloran obtained her BSc in applied physics from the University of Limerick, Ireland, in 2008. In 2013, she received her PhD from the School of Physics, National University of Ireland, Galway.

Eamonn O' Donoghue is a consultant opthalmic surgeon at University Hospital Galway, Ireland.

Chris Dainty is a professorial research associate at UCL Institute of Ophthalmology, London, and a professor Emeritus at the National University of Ireland, Galway. He coauthored, with Rodney Shaw, the text "Image Science" in 1974, has coauthored more than 180 peer-reviewed papers, and supervised 65 PhD students to completion. He has been given numerous awards for his research leadership and is a member of the Royal Irish Academy. From 1990 to 1993, he was president of The International Commission for Optics and was 2011 president of OSA.